

Supporting Information for:

## A Visible Fluorescent Light-up Probe for DNA Three-Way Junctions Provides Host-Guest Biosensing Applications.

Abigail J. Van Riesen,<sup>†</sup> Jennifer Le,<sup>†</sup> Sladjana Slavkovic,<sup>‡</sup> Zachary R. Churcher,<sup>‡</sup>

Aron A. Shoara,<sup>‡</sup> Philip E. Johnson<sup>‡,\*</sup> and Richard A. Manderville<sup>†,\*</sup>

<sup>†</sup>Departments of Chemistry and Toxicology, University of Guelph, Guelph, Ontario, Canada N1G 2W1

<sup>‡</sup>Department of Chemistry, York University, 4700 Keele Street, Toronto, Ontario, Canada M3J 1P3

### Corresponding Authors

P.E.J. e-mail: pjohnson@yorku.ca

R.A.M. e-mail: rmanderv@uoguelph.ca

### Table of Contents:

1. <b>Figure S1.</b> UV-vis $pK_a$ determination for FPhOBtz.	<b>S2</b>
2. <b>Figure S2.</b> Solvatochromism and $E_T(30)$ correlation for FPhOBtz.	<b>S2</b>
3. <b>Figure S3.</b> pH-influence on fluorescence intensity of FPhOBtz•MN4.	<b>S3</b>
4. <b>Figure S4.</b> ITC thermogram for quinine binding to MN4.	<b>S3</b>
5. <b>Figure S5.</b> ITC thermogram for cholic acid binding to CABA.	<b>S4</b>
6. <b>Figure S6.</b> NOESY spectrum of MN4.	<b>S4</b>
7. <b>Figure S7.</b> Histogram of $^1H$ NMR chemical shifts of free and bound MN4.	<b>S5</b>
8. <b>Figure S8.</b> Fluorescence titration of target-mediated displacement from 3WJs.	<b>S5</b>
9. <b>Figure S9.</b> Determination of LoD and LoQ.	<b>S6</b>
10. <b>Figure S10.</b> ITC-based competition binding experiments.	<b>S7</b>
11. <b>Table S1.</b> ITC-Competition experiment results.	<b>S7</b>
12. <b>Figure S11.</b> $I_{rel}$ for FPhOBtz binding to various DNA/RNA samples.	<b>S8</b>
13. <b>Figure S12.</b> Target-mediated displacement by estradiol and DCA.	<b>S9</b>
14. <b>Figure S13.</b> Detection of quinine in human serum.	<b>S10</b>
15. <b>Figure S14.</b> Detection of cocaine in human serum.	<b>S11</b>
16. <b>Figure S15.</b> Detection of cholic acid in human serum.	<b>S11</b>
17. <b>Figure S16.</b> $^1H$ NMR spectrum of FPhOBtz in DMSO- $d_6$ .	<b>S12</b>
18. <b>Figure S17.</b> $^{13}C$ NMR spectrum of FPhOBtz in DMSO- $d_6$ .	<b>S12</b>
19. <b>Figure S18.</b> Positive-Ionization HRMS of FPhOBtz.	<b>S13</b>

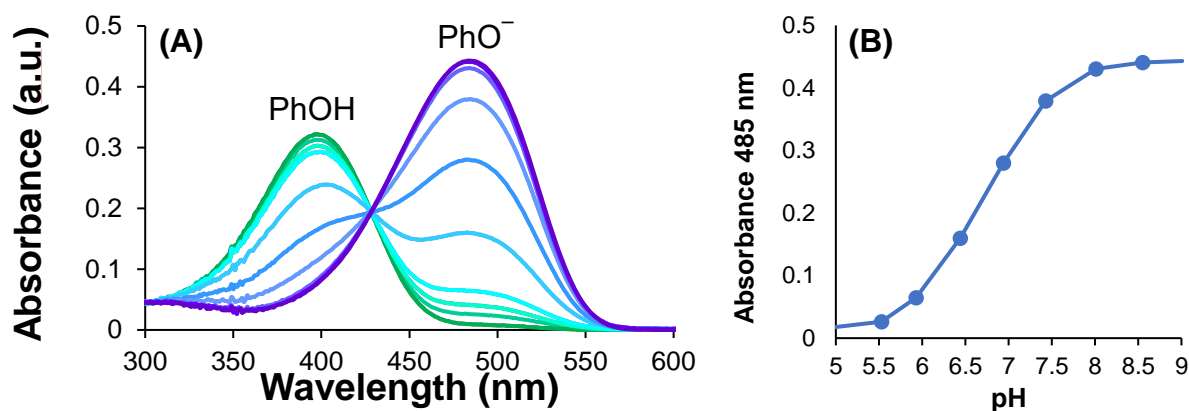


**Figure S1.** (A) UV-vis absorption spectra of FPhOBtz (10  $\mu$ M) as a function of pH in aqueous buffer (0.05 M containing 0.2 M KCl) at 21  $^{\circ}$ C and (B) a plot of phenolate absorbance at 485 nm as a function of pH;  $pK_a = 6.6 \pm 0.05$ .

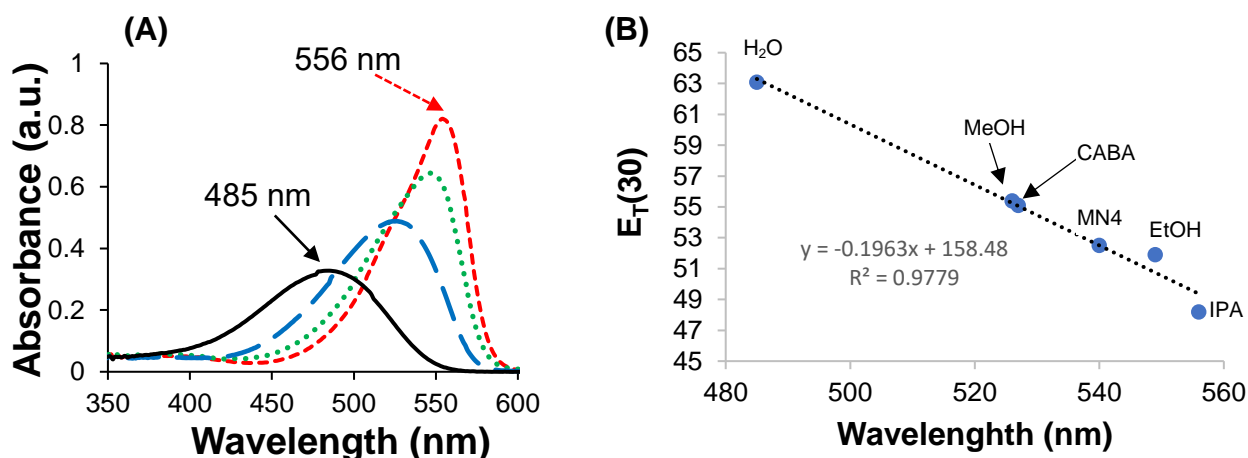


**Figure S2.** (A) UV-vis spectra of FPhOBtz (10  $\mu$ M) in H<sub>2</sub>O (solid black trace,  $\lambda_{max} = 485$  nm,  $\epsilon = 32,787$  cm<sup>-1</sup>M<sup>-1</sup>), MeOH (dashed blue trace,  $\lambda_{max} = 526$  nm,  $\epsilon = 48,864$  cm<sup>-1</sup>M<sup>-1</sup>), EtOH (dotted green trace,  $\lambda_{max} = 549$  nm,  $\epsilon = 64,428$  cm<sup>-1</sup>M<sup>-1</sup>) and IPA (dashed red trace,  $\lambda_{max} = 556$  nm,  $\epsilon = 82,077$  cm<sup>-1</sup>M<sup>-1</sup>). (B) Plot of  $\lambda_{max}$  for FPhOBtz in nm versus the empirical solvent polarity scale  $E_T(30)$  in kcal/mol. From the plot, the  $E_T(30)$  value for MN4 is  $\sim 52.5$  kcal/mol, while the value for CABA is  $\sim 55.1$  kcal/mol.

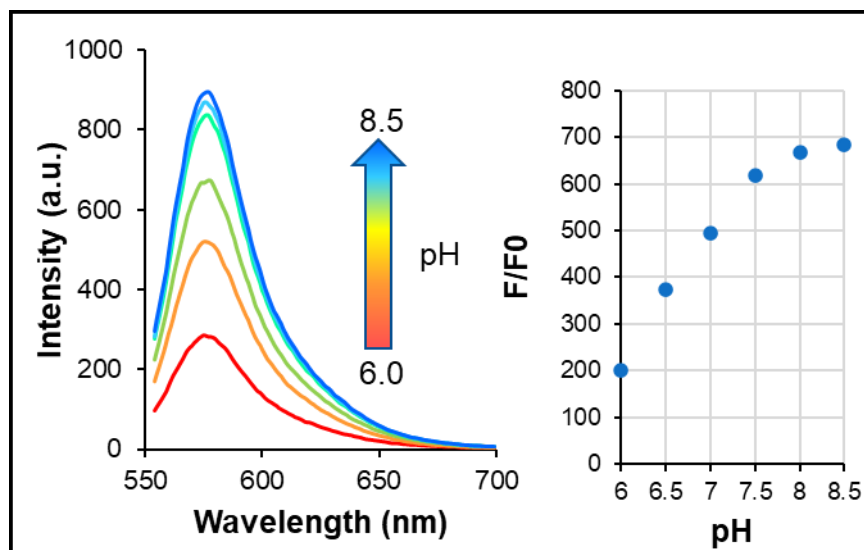


**Figure S3.** Fluorescence response of FPhOBtz (1  $\mu$ M) to binding MN4 (2 equiv.) as a function of pH highlighting the greater emission intensity response by the phenolate of the dye. Solutions were prepared in PBS at pH values from 6.0-8.5 at 25  $^{\circ}$ C.

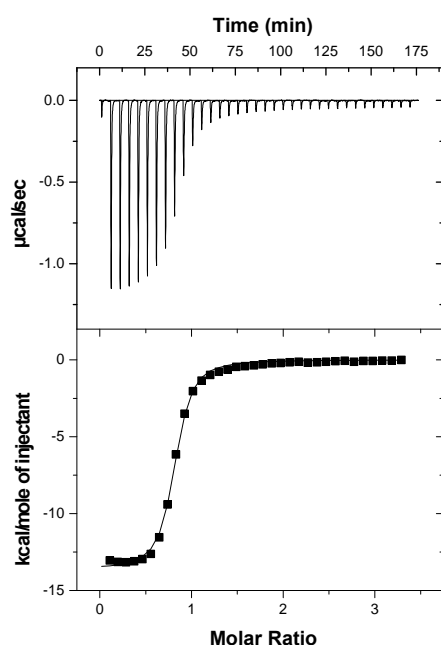


**Figure S4.** ITC thermogram for quinine binding to MN4. On top is the raw titration data showing the heat resulting from each injection of ligand into aptamer solution. The bottom shows the integrated heat plot after correcting for the heat of dilution. Data for the cocaine-binding aptamer was acquired in 20 mM Tris (pH 7.4), 140 mM NaCl, 5 mM KCl,) at 15 $^{\circ}$ C.

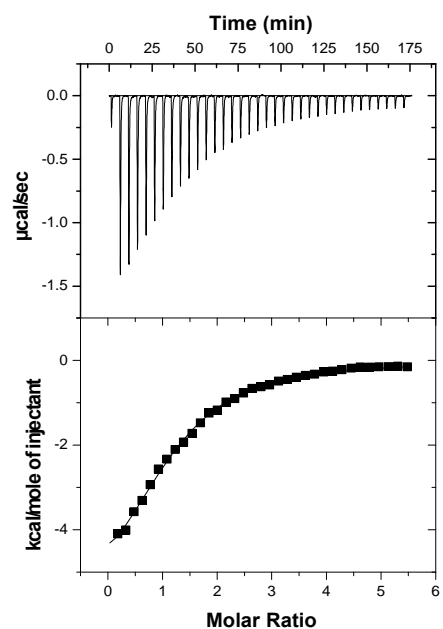


**Figure S5.** ITC thermogram for cholic acid binding to CABA. On top is the raw titration data showing the heat resulting from each injection of ligand into aptamer solution. The bottom shows the integrated heat plot after correcting for the heat of dilution. Data was acquired in PBS (pH 7.4) at 15°C.

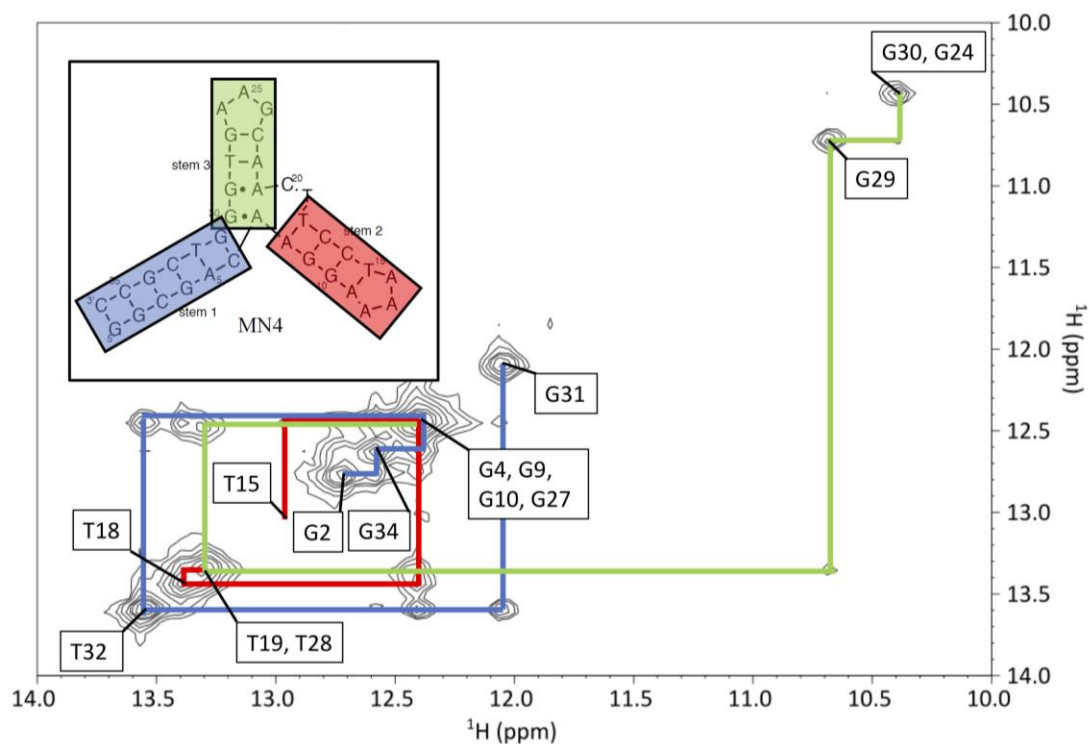


**Figure S6.** 2D <sup>1</sup>H-<sup>1</sup>H NOESY spectrum of the FPhOBtz-bound MN4 cocaine-binding aptamer. Spectrum shows the imino-imino cross peaks used to assign the FPhOBtz-bound MN4 aptamer. Spectra were acquired with an aptamer concentration of 1.4 mM, in 140mM NaCl, 10mM Na<sub>2</sub>HPO<sub>4</sub>, pH 6.8, 10% <sup>2</sup>H<sub>2</sub>O-90% H<sub>2</sub>O at 5°C.

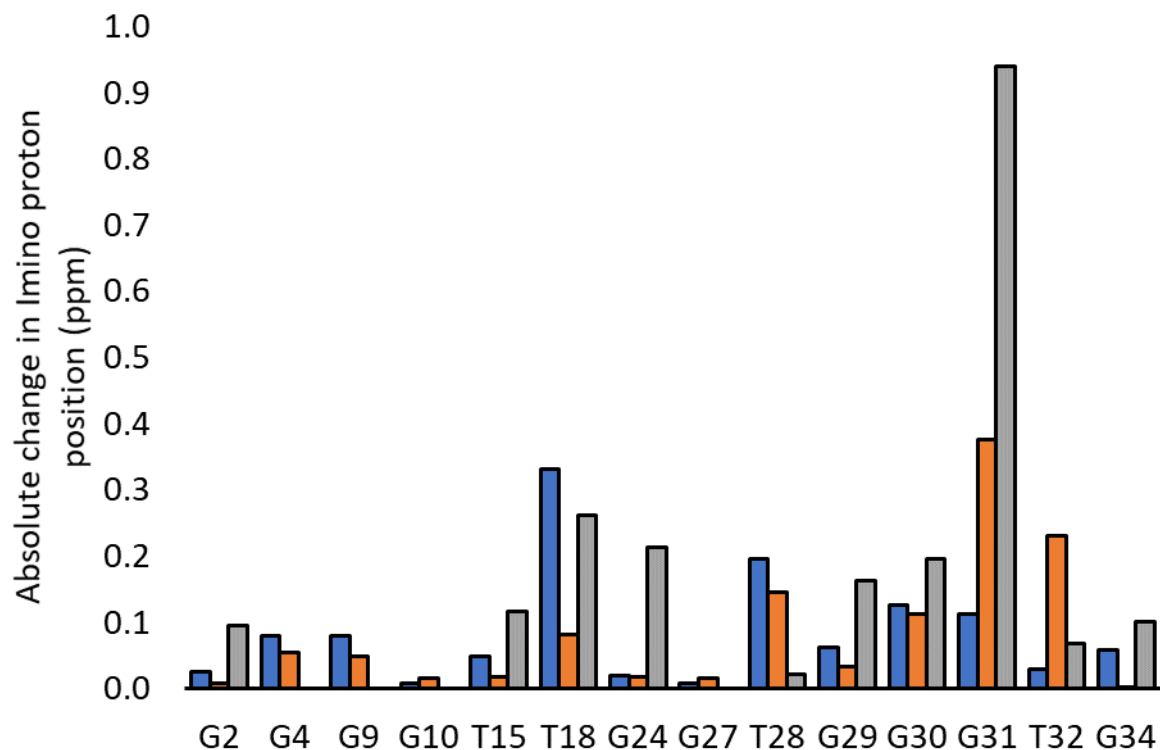


**Figure S7.** Histogram showing the change in  $^1\text{H}$  NMR chemical shift between free and bound MN4 cocaine-binding aptamer  $|\delta_{\text{bound}} - \delta_{\text{free}}|$ . This comparison was done for MN4 bound to FPhOBt (blue), cocaine (orange), and quinine (grey).

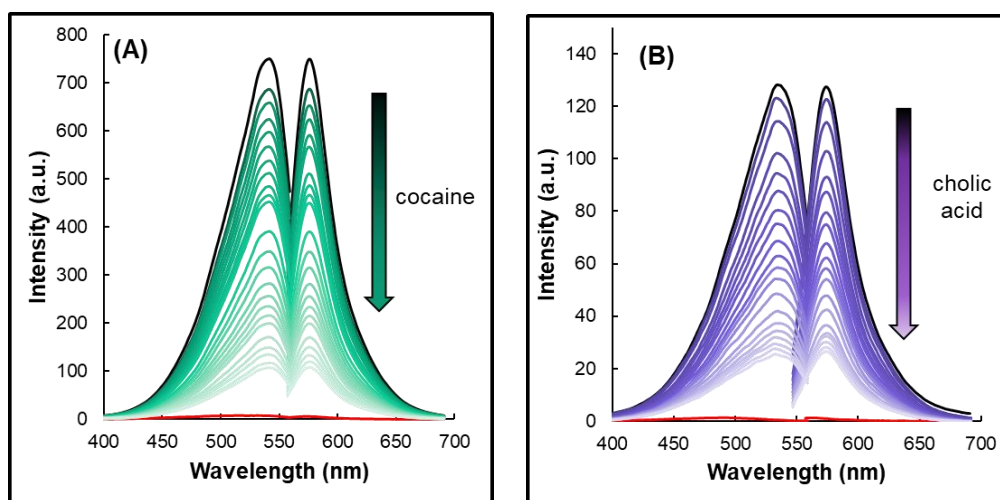


**Figure S8.** Fluorescence titration of target-mediated displacement of FPhOBt ( $1\ \mu\text{M}$ ) from: (A) MN4 ( $2\ \mu\text{M}$ ) by  $100\ \mu\text{M}$  cocaine, and (B) CABA ( $2\ \mu\text{M}$ ) by  $50\ \mu\text{M}$  cholic acid. Titrations were carried out in PBS pH 7.4 at  $25\ ^\circ\text{C}$ . Fluorescence of free FPhOBt is indicated by the red trace in (A) and (B).

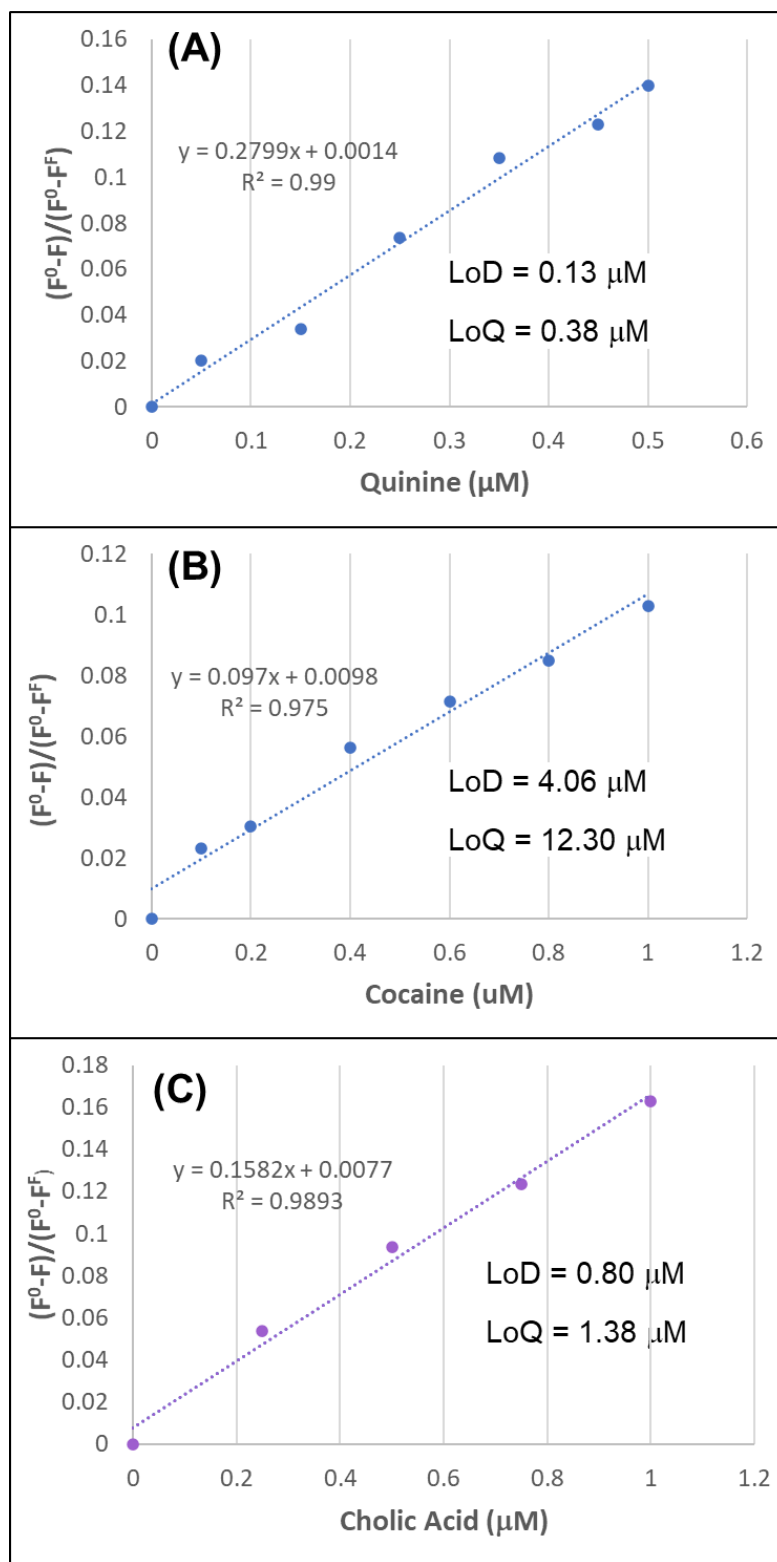


**Figure S9** Determination of Limits of Detection (LoD) and quantification (LoQ) for quinine (A), cocaine (B) and cholic acid (C) binding to the cocaine-binding aptamer MN4 ((A) and (B)) and CABA (C) by displacing FPhOBtz (Fluorescence Titration data, Figure 7 in main text).

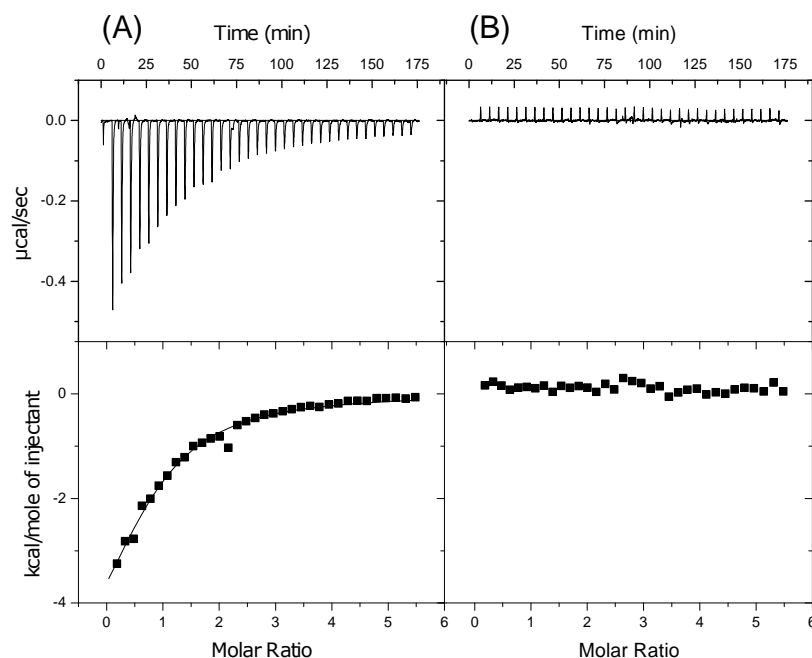


**Figure S10.** ITC-based competition binding experiments. Shown is the interaction of (A) cholic acid-bound CABA with FPhOBtz and (B) FPhOBtz-bound CABA with cholic acid. On top of each thermogram is the raw titration data showing the heat resulting from each injection of ligand into aptamer solution. On the bottom is the integrated heat plot after correcting for the heat of dilution. The fit line in (A) is from using the competitive binding model. All binding experiments were performed at 15 °C in a PBS buffer (pH 7.4) containing 0.6% DMSO.

**Table S1.** Competition experiment results

MN4 cocaine-binding aptamer			
	$K_d$ ( $\mu\text{M}$ )	$\Delta H$ ( $\text{kcal mol}^{-1}$ )	$-T\Delta S$ ( $\text{kcal mol}^{-1}$ )
MN4-dye, titrate quinine	$0.11 \pm 0.03$	$-11 \pm 1$	$1.6 \pm 0.2$
MN4-quinine, titrate dye		NB	
Cholic acid binding aptamer (CBA)			
CBA-cholate, titrate dye	$3 \pm 1$	$-11 \pm 1$	$4.6 \pm 0.1$
CBA-dye, titrate cholate		NB	
NB indicates no binding detected. Data were fit to a competitive binding model.			

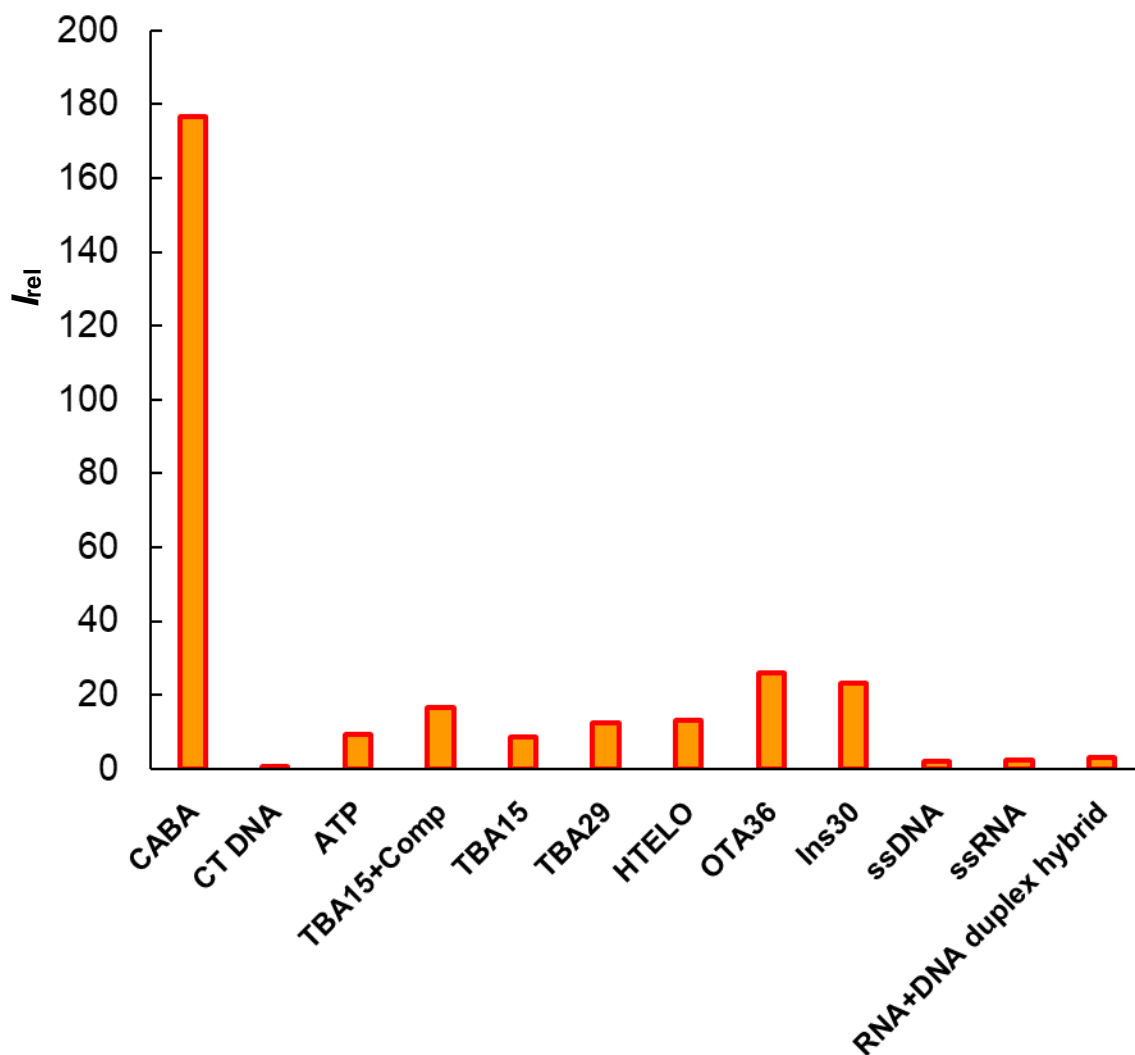


**Figure S11.** Fluorescence response ( $I_{rel}$ ) of FPhOBtz (1  $\mu$ M) to various DNA samples (2 equiv.) compared to its  $I_{rel}$  for CABA binding in PBS pH 7.4 at 25 °C.



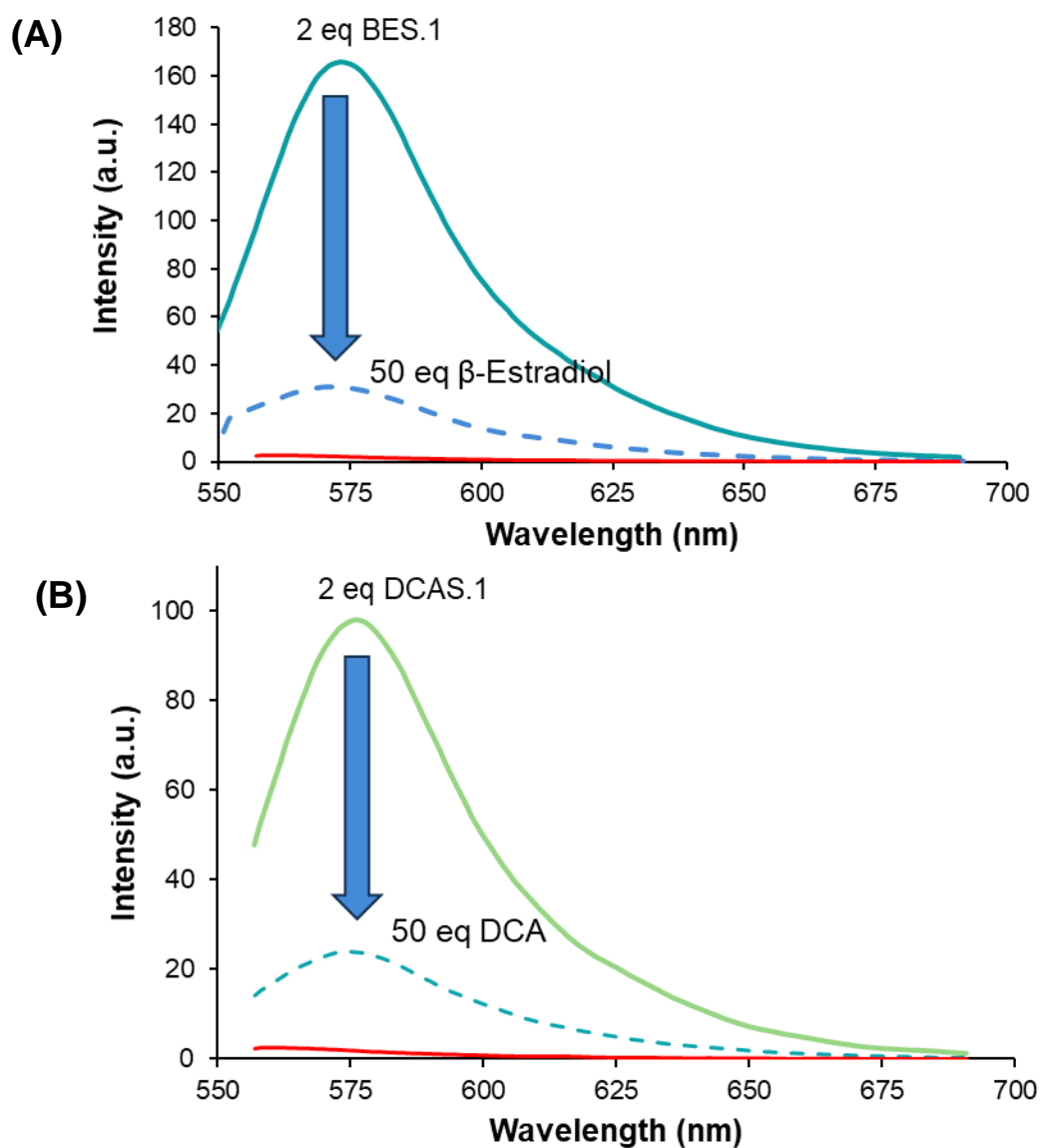


**Figure S12.** Target-mediated displacement of FPhOBtz ( $1.7 \mu\text{M}$ ) from: (A) BES.1 ( $2 \mu\text{M}$ ) by  $50 \mu\text{M}$  estradiol, and (B) DCAS.1 ( $2 \mu\text{M}$ ) by  $50 \mu\text{M}$  DCA carried out in PBS pH 7.4 at  $25^\circ\text{C}$ . Fluorescence of free FPhOBtz is indicated by the red trace in (A) and (B).

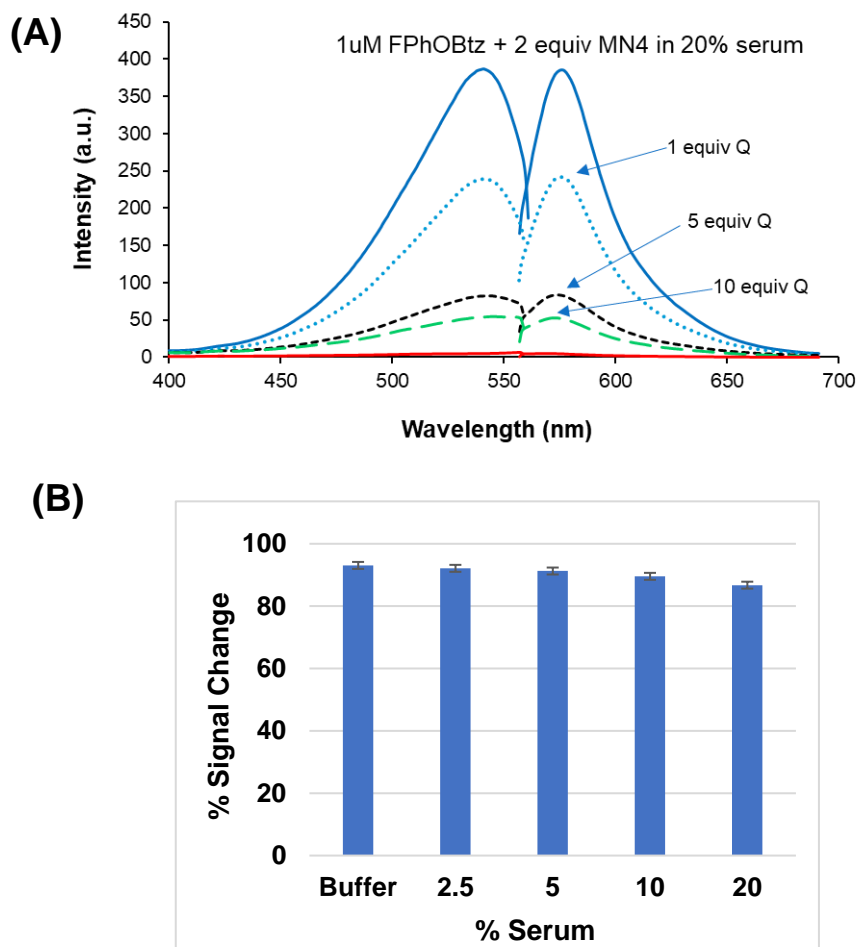


**Figure S13.** (A) FPhOBtz (1  $\mu$ M) emission response to MN4 (2 equiv.) binding in 20% serum and subsequent loss in emission through quinine (Q) binding at 1, 5 and 10 equiv. (B) Detection of quinine spiked into different concentration (0%, 2.5%, 5%, 10%, and 20%) of serum with MN4. Signal change decreases slightly with increasing concentrations of serum. Error bars represent the standard deviation of three measurements. Experimental conditions: [MN4] = 2  $\mu$ M, [FPhOBtz] = 1  $\mu$ M and [quinine] = 10  $\mu$ M. The signal change is calculated as  $1 - (F_{\text{quinine}} - F_{\text{FPhOBtz}} - F_{\text{background}}) / (F_{\text{FPhOBtz}} - F_{\text{background}})$  where the background is derived from FPhOBtz in the serum sample.

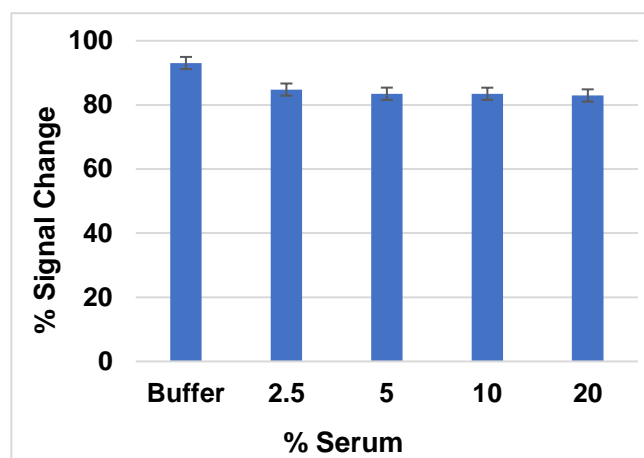


**Figure S14.** Successful detection of cocaine spiked into different concentration (0%, 2.5%, 5%, 10%, and 20%) of serum with MN4. Signal change decreases slightly with increasing concentrations of serum. Error bars represent the standard deviation of three measurements. Experimental conditions: [MN4] = 2  $\mu$ M, [FPhOBtz] = 1  $\mu$ M and [cocaine] = 100  $\mu$ M. The signal change is calculated as  $1 - (F_{\text{cocaine}} - F_{\text{FPhOBtz}} - F_{\text{background}}) / (F_{\text{FPhOBtz}} - F_{\text{background}})$  where the background is derived from FPhOBtz in the serum sample.

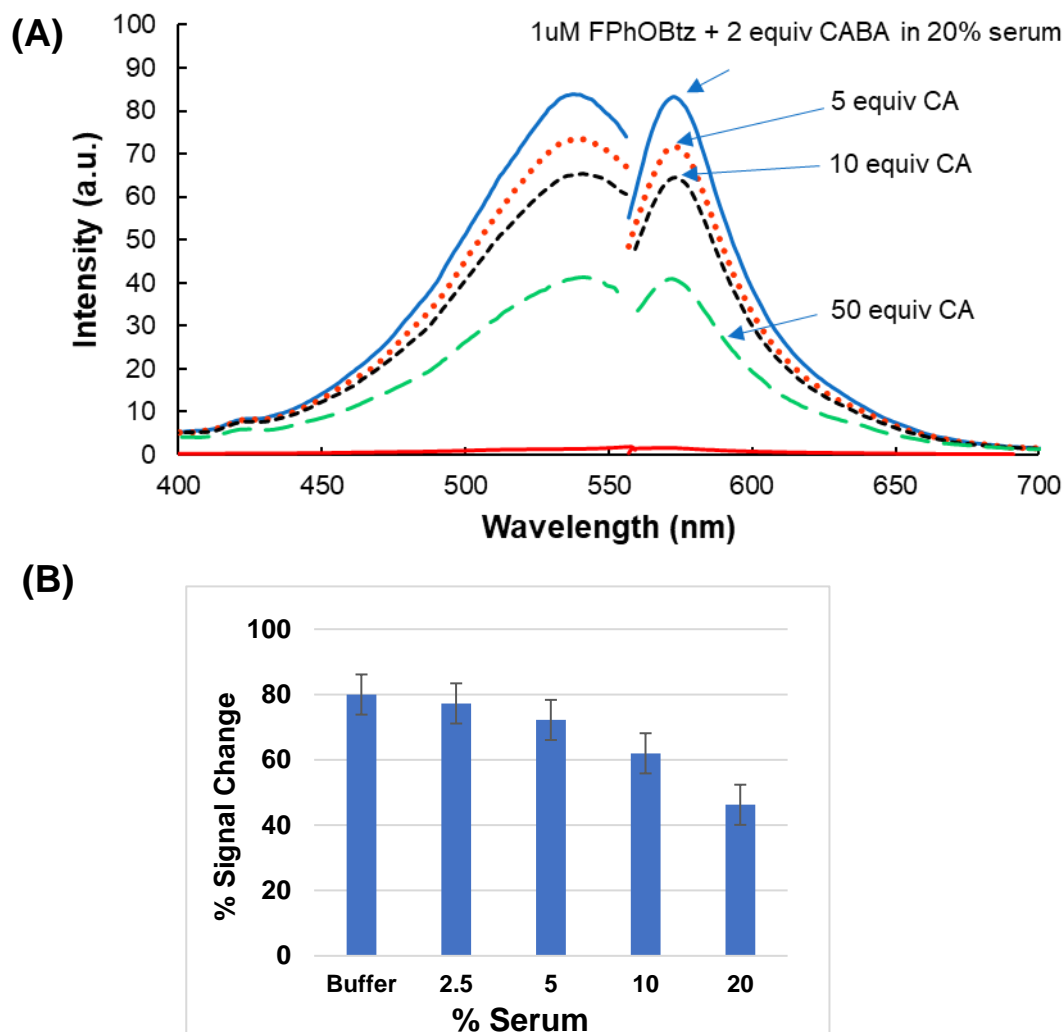


**Figure S15.** (A) FPhOBtz (1  $\mu\text{M}$ ) emission response to CABA (2 equiv.) binding in 20% serum and subsequent loss in emission through cholic acid (CA) binding at 5, 10 and 50 equiv. (B) Successful detection of cholic acid spiked into different concentration (0%, 2.5%, 5%, 10%, and 20%) of serum with CABA. Signal change decreases slightly with increasing concentrations of serum. Error bars represent the standard deviation of three measurements. Experimental conditions: [CABA] = 2  $\mu\text{M}$ , [FPhOBtz] = 1  $\mu\text{M}$  and [cholic acid] = 50  $\mu\text{M}$ . The signal change is calculated as  $1 - (F_{\text{cholic acid}} - F_{\text{FPhOBtz}} - F_{\text{background}}) / (F_{\text{FPhOBtz}} - F_{\text{background}})$  where the background is derived from FPhOBtz in the serum sample.

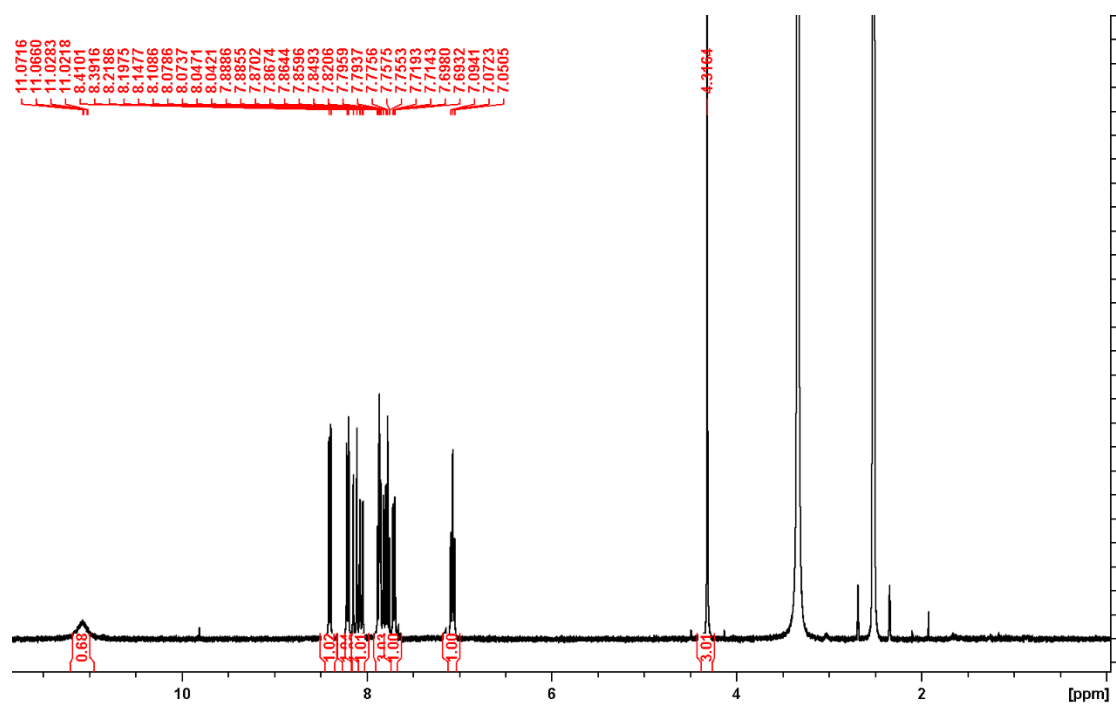


**Figure S16.** <sup>1</sup>H NMR spectrum of FPhOBtz in DMSO-d<sub>6</sub>.

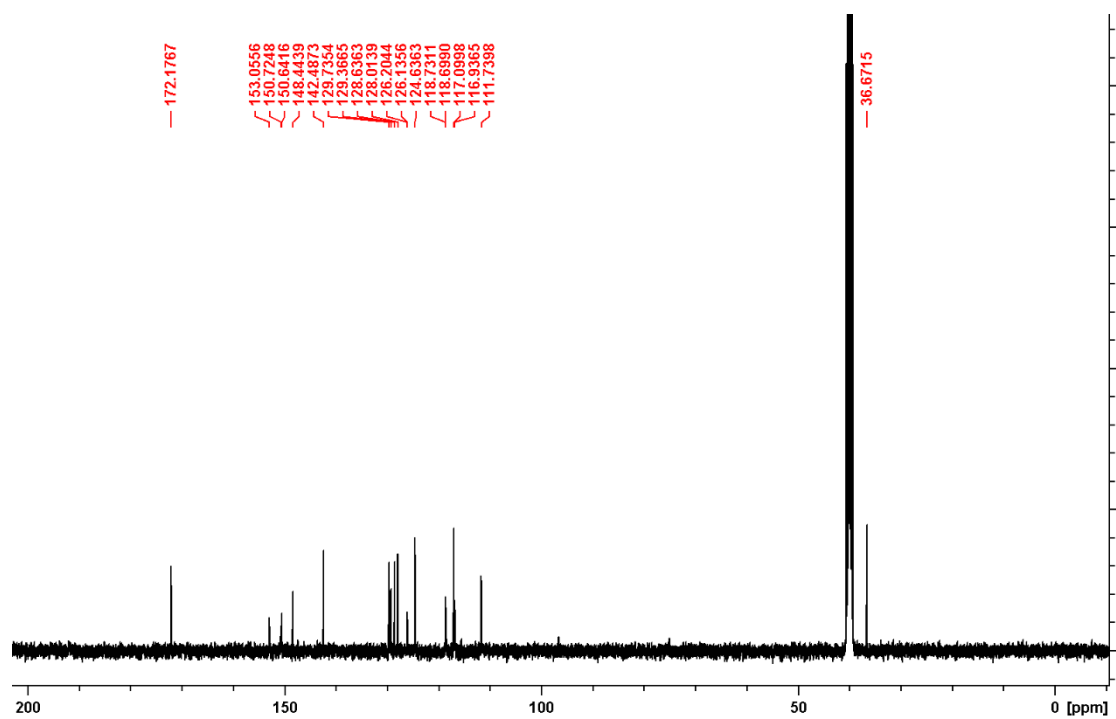


**Figure S17.** <sup>13</sup>C NMR spectrum of FPhOBtz in DMSO-d<sub>6</sub>.

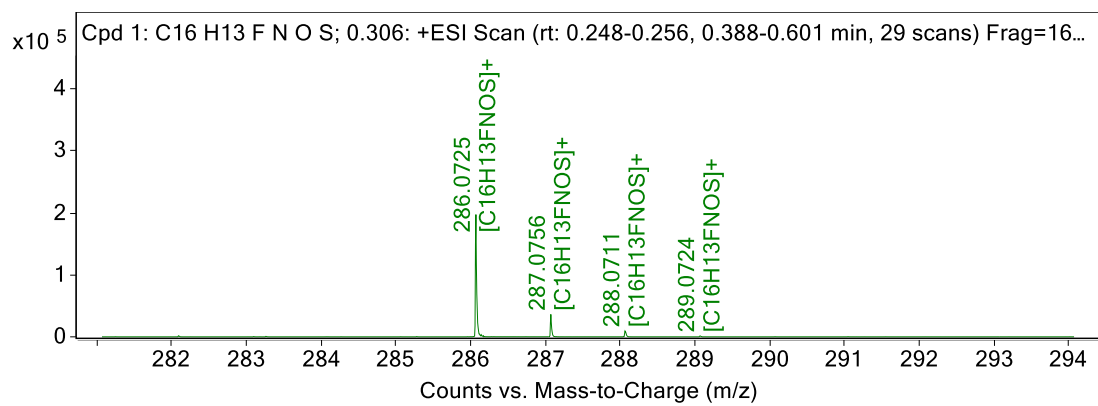


**Figure S18.** Positive-Ionization HRMS of FPhOBtz.